

Electrically tunable lasing from a dye-doped two-dimensional hexagonal photonic crystal made of holographic polymer-dispersed liquid crystals

D. Luo,¹ X. W. Sun,^{1,2,a)} H. T. Dai,¹ H. V. Demir,¹ H. Z. Yang,³ and W. Ji³

¹School of Electrical and Electronic Engineering, Nanyang Technological University, Nanyang Avenue, Singapore 639798

²Department of Applied Physics, Tianjin University, Tianjin 300072, People's Republic of China

³Department of Physics, National University of Singapore, 2 Science Drive 3, Singapore 117542

(Received 24 June 2010; accepted 5 August 2010; published online 23 August 2010)

Mode-dependent electrically tunable lasing of transverse electric (TE) and transverse magnetic (TM) modes is demonstrated in a dye-doped two-dimensional hexagonal photonic crystal made of holographic polymer-dispersed liquid crystals (LCs). Over 10 nm redshifting in lasing with multiple peaks in nonpolarizing spectra is obtained by applying external voltages up to 40 V. The splitting of lasing spectra between two perpendicular polarizations with the applied voltage is observed, which can be explained through the difference in effective refractive index of LC droplet change with the applied electric field for TE and TM modes. © 2010 American Institute of Physics.

[doi:10.1063/1.3483234]

Holographic polymer-dispersed liquid crystals (H-PDLCs) have received much attention because of their electrically switchable/tunable properties.¹ Thus far, two-dimensional (2D) and three-dimensional (3D) photonic crystals (PCs) have been demonstrated.^{2,3} H-PDLC-based lasing has also recently been investigated in one-dimensional (1D) dye-doped reflection and transmission gratings,^{4,5} where the underlying mechanism is much similar to conventional 1D distributed feedback (DFB) lasers,⁶ and 2D dye-doped PC with square⁷ and hexagonal^{8,9} lattices, where the group-velocity anomaly¹⁰ is responsible for local field enhancement. The group-velocity anomaly, where the group velocity is significantly slowed down over a wide range of wave vectors, is peculiar to 2D and 3D PCs and even exists in PCs based on H-PDLC materials with rather small index contrast.

Recently, the electrically tunable properties of lasing based on dye-doped H-PDLC have been demonstrated in reflection grating,^{11,12} transmission grating,^{5,13} and 2D square PC.⁸ The electrical erasing and shifting in lasing in H-PDLC have also been discussed. However, the polarization characteristics of lasing under applied voltage have not been investigated yet, especially in 2D PC. Under applied voltage, the refractive index contrasts of 2D PC for the two perpendicular

polarizations change differently with respect to each other because of the realignment of the nematic directors in the LC droplets along the electric field, which possibly leads to different lasing spectra corresponding to transverse electric (TE) and transverse magnetic (TM) modes. Previously, we reported experimental lasing results both from Γ X and Γ M directions in a dye-doped 2D H-PDLC PC.⁹ In this paper, we should demonstrate the electrically tunable property of lasing for TE and TM modes in a dye-doped 2D H-PDLC PC with hexagonal lattice. The splitting of laser spectra between TE and TM modes is observed and subsequently explained by the opposite band shifting in TE and TM modes.

In our experiment, the LC/prepolymer mixture syrup that is used to fabricate the dye-doped 2D PC with hexagonal lattice structure consisted of 63.76 wt % monomer, trimethylolpropane triacrylate, 7.05 wt % cross-linking monomer, *N*-vinylpyrrolidone, 0.49 wt % photoinitiator, Rose Bengal, 0.98 wt % coinitiator, *N*-phenylglycine, 9.30 wt % surfactant, octanoic acid, and 1.18 wt % lasing dye, 4-dicyanomethylene-2-methyl-6-p-dimethylaminostyryl-4H-pyran, all from Sigma-Aldrich, and 17.24 wt % LC, E7 ($n_o=1.5216$ and $n_e=1.7462$), from Merck. The mixture was sandwiched in a cell, which was formed by two pieces of

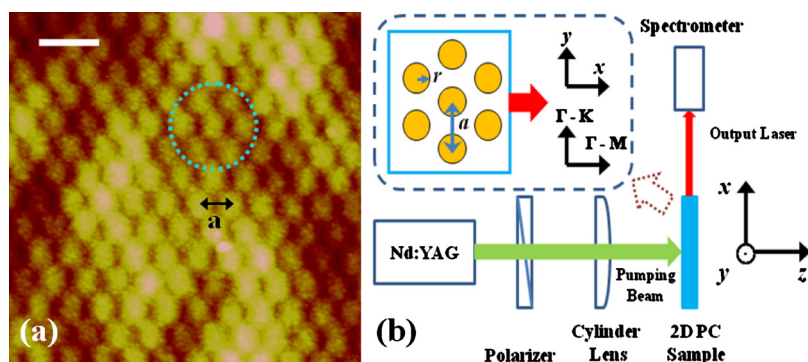


FIG. 1. (Color online) (a) AFM image showing the surface morphology of a 2D hexagonal H-PDLC PC, a is the lattice constant. Scale bar: 1 μm . (b) Schematic optical setup of the lasing experiment.

^{a)}Author to whom correspondence should be addressed. Electronic mail: exwsun@ntu.edu.sg.

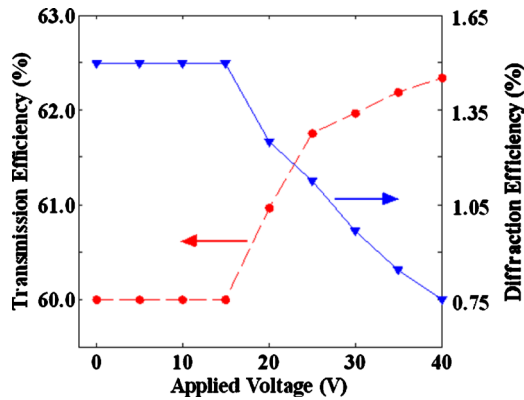


FIG. 2. (Color online) Changes in transmission and diffraction efficiency of our 2D H-PDLC PC sample as functions of applied voltage.

indium tin oxide coated glass. The cell gap $d=7 \mu\text{m}$.

The 2D H-PDLC PC with hexagonal lattice structure was holographically fabricated through the three-beam interference based on a single prism using collimated Ar+laser beam (514.5 nm). The exposure intensity of each beam was $5 \text{ mW}/\text{cm}^2$, with an exposure time of 120 s. The recording area of the fabricated 2D PC sample was about $5 \times 5 \text{ mm}^2$ in x - y plane. During the polymerization process, monomers start to photopolymerize in high intensity regions while LCs diffuse into low intensity region, thus forming the columnar polymer and LC droplets after the phase separation.

Figure 1(a) shows the surface morphology of the 2D H-PDLC PC with a hexagonal lattice structure imaged by an atomic force microscope (AFM). The lattice constant of the 2D PC sample, a , was $\sim 515 \text{ nm}$ and the polymer columns have a radius of $\sim 152 \text{ nm}$. The lattice constant in x - y plane can be calculated by $a=2\lambda/(3n \sin \theta)$. In our experiments, $\lambda=514.5 \text{ nm}$, $n=1.535$ (calculated according to the ratio of polymer and LC), and $\theta=25.3^\circ$, the theoretical lattice constant is about 523 nm. The detail fabrication experiment can be found elsewhere.⁹ Considering a general 5% volume shrinkage for acrylate monomers during photopolymerization,¹⁴ the experimental lattice constant (515 nm) was in good agreement with our prediction (523 nm).

The schematic optical setup of our lasing experiment is shown in Fig. 1(b). To generate lasing from the 2D H-PDLC sample, a Q-switched frequency-doubled Nd:yttrium-aluminum-garnet pulsed laser operating at 532 nm, with a pulse duration of 7 ns, and a repetition rate of 10 Hz, was

used. A linearly polarized (electric field in y direction) pumping laser, focused by a cylinder lens, was incident on the surface of the sample along the z direction. A fiber coupled spectrometer positioned along ΓM direction with a resolution of 0.6 nm was used to collect output lasing beams. The experiment was performed at room temperature (25°C).

Figure 2 shows the changes in transmission and diffraction efficiency of our 2D H-PDLC PC sample (with incident angle $\sim 40^\circ$, where the incident angle is defined as the angle between the probe laser propagation direction and the normal line of glass-substrate-plane) as functions of applied voltage. A linear polarized white light (polarization direction along y axis) was used as illuminate source. There was no significant difference of transmission and diffraction efficiency among incident lights with different polarizations in x - y plane. The threshold behavior was observed at 15 V.

Figures 3(a)–3(c) show the lasing spectra from ΓM direction of our 2D PC sample at the externally applied voltages of 0 V, 25 V, and 40 V, respectively, all with optical pumping energy of $380 \mu\text{J}/\text{pulse}$. The green curves represent the lasing spectra obtained without polarizer, and their corresponding lasing peaks are 613/617 nm, 622/627 nm, and 625/631 nm under 0 V, 25 V, and 40 V, respectively. Those lasing peaks were due to the group-velocity anomalies, which are peculiar to 2D and 3D PCs. The simulation works reported by Sakoda¹⁰ indicated that two or more lasing peaks can be generated simultaneously in the frequency range of group-velocity anomalies of 2D PC with a small index contrast, which gives a good explanation of our experimental spectra with multilasing peaks here. Additionally, these competing lasing peaks tend to appear at high pumping energy levels, which could be due to the spatial hole burning effect.¹⁵ In our experiment, over 10 nm redshifting in the nonpolarized lasing wavelength with the increased voltage was obtained.

The directors of the LC droplets in H-PDLC will be aligned by external electric field, which produces a larger difference in the PC band structure of TE and TM modes and finally leads to different laser spectra for them. In Fig. 3, the laser spectra of TE and TM modes are represented by red and blue curves, respectively. From Fig. 3(a), we can see that the lasing spectra show no significant difference for TE and TM modes, as the peaks of 613/617 nm in nonpolarized spectra are reserved both in TE and TM case. When the external voltage applied exceeded the threshold of 15 V [as shown in

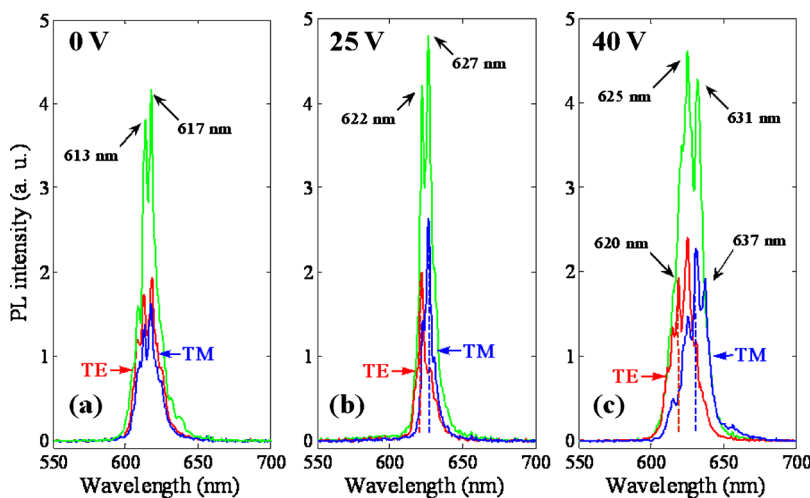


FIG. 3. (Color online) Lasing spectra measured along ΓM directions under the applied voltage of (a) 0 V, (b) 25 V, and (c) 40 V.

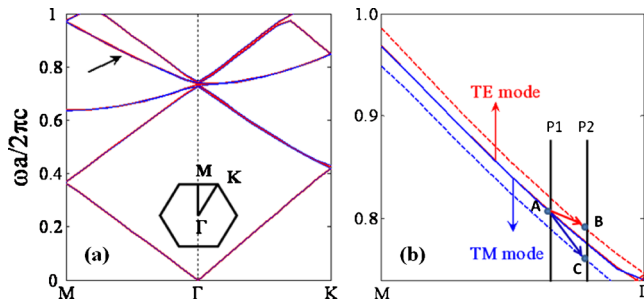


FIG. 4. (Color online) Photonic band structure of the 2D hexagonal H-PDLC PC. The solid lines represent the TE and TM modes, respectively. (b) The shift in the band under increasing applied voltage. The arrows represent the shifting directions.

Figs. 3(b) and 3(c)], two phenomena are observed: First, the lasing splitting spectra of TE and TM modes started to appear and enlarged as the voltage increased. Second, the lasing spectrum of TE and TM modes redshifted as the voltage increased.

To further investigate the lasing in dye-doped 2D H-PDLC PC, the photonic band structures were calculated for the 2D hexagonal HPDLC PC using the plane wave expansion method,¹⁶ shown in Fig. 4(a). Here the band structures of TE and TM modes are represented by red and blue solid line, respectively, where $r=0.30a$, $n_p=1.522$, and $n_{LC}=1.597$. The tunable lasing described in Fig. 3 ranges from 613 to 637 nm, corresponding to the normalized frequency range from $\omega a/2\pi c=0.808$ to 0.840 along ΓM direction. The band where laser actions occurred is marked by the arrow. It is noticed that the index contrast is quite small in our 2D PC sample, therefore leading to the strong overlap of the TE and TM band structures [as shown in Fig. 4(a)], which leads to the nonsplit lasing spectra of TE and TM modes when no voltage is applied.

However, when an external voltage was applied, the effective index of LC droplets started to decrease for TE mode and increase for TM mode, leading to the index contrast of LC droplets and polymer decrease and increase for TE and TM modes, respectively.⁸ Figure 4(b) shows the shifting trend of the band with increasing external applied voltage. The decreasing and increasing of effective refractive index for TE and TM modes yields the upward shifting for the band of TE mode (red dashed line) and downward shifting for the band of TM mode (blue dashed line), which in turn leads to the relatively shorter wavelength of lasing peaks in TE mode and longer wavelength of lasing peaks in TM mode, as shown in Figs. 3(b) and 3(c). The shift directions of TE and TM bands are shown by the arrows. Therefore, in the presence of an external voltage, the directors of the LC droplets in H-PDLC will be aligned, which produces the larger difference of PC band structure for TE and TM mode, from opposite band shift directions, and finally leading to the different lasing spectra for TE and TM modes.

If applied voltage further increases, the band difference of TE and TM modes will become bigger (not shown here), due to the further decreased and increased effective index of LC for TE and TM mode, respectively. It means the splitting spacing of peaks for TE and TM modes will increase with the increased electric field. From Fig. 3(a), we can see that at voltage of 0 V, the laser peaks of TE and TM modes are overlapped, no splitting; In Fig. 3(b), at voltage of 25 V, the spacing of peaks for TE and TM modes (distance of dashed

red and blue lines) is $(627-622) \text{ nm}=5 \text{ nm}$. In Fig. 3(c), at voltage of 40 V, the spacing of peaks could be considered as the difference of central peaks for TE and TM modes (distance of dashed red and blue lines); $(631-620) \text{ nm}=11 \text{ nm}$. Therefore, the splitting spacing of the peaks for the TE and TM modes is increased as the increasing electric field, consistent with the prediction from photonic band.

For the redshift in lasing spectrum both for TE and TM modes as the voltage increased in our experiment, the possible reason is as follows: because of the property of lasing induced from group velocity anomaly, the possible range of lasing frequencies is within the photonic band, which means that the generated laser peaks could be different under different specific oscillation conditions (e.g., different voltages). Assuming the oscillation is initially at P1 position (with lasing point A on the band) without voltage [shown in Fig. 4(b)]. When voltage is applied, the condition changes corresponding and the oscillation position might be shifted to P2, accompanied by the split of TE and TM band (with lasing point B on TE and point C on TM band). Therefore, the movement from P1 to P2 and the split of TE and TM with voltage applied lead to following two results: (1) comparing to point A, the laser wavelengths on points B and C are larger in absolute value, meaning a redshift in lasing spectrum; (2) the split of points B and C leads to the laser splitting for TE and TM modes.

In conclusion, we demonstrated the electrically tunable properties of lasing with multi-peaks from a dye-doped 2D H-PDLC PC with hexagonal lattice. Over 10 nm redshifting in the lasing peaks were obtained in nonpolarization spectra when the applied voltage was increased up to 40 V. The effect of the applied electric field on the effective refractive index of LC are, however, also different for the TE and TM modes, which lead to a opposite band shifting and eventually result in the splitting of the lasing spectra between TE and TM modes.

¹T. J. Bunning, L. V. Natarajan, V. P. Tondiglia, and R. L. Sutherland, *Annu. Rev. Mater. Sci.* **30**, 83 (2000).

²Y. J. Liu and X. W. Sun, *Appl. Phys. Lett.* **89**, 171101 (2006).

³R. L. Sutherland, V. P. Tondiglia, L. V. Natarajan, S. Chandra, D. Tomlin, and T. J. Bunning, *Opt. Express* **10**, 1074 (2002).

⁴G. S. He, T.-C. Lin, V. K. S. Hsiao, A. N. Cartwright, P. N. Prasad, L. V. Natarajan, V. P. Tondiglia, R. Jakubiak, R. A. Vaia, and T. J. Bunning, *Appl. Phys. Lett.* **83**, 2733 (2003).

⁵R. Jakubiak, L. V. Natarajan, V. Tondiglia, G. S. He, P. N. Prasad, T. J. Bunning, and R. A. Vaia, *Appl. Phys. Lett.* **85**, 6095 (2004).

⁶H. Kogelnik and C. V. Shank, *J. Appl. Phys.* **43**, 2327 (1972).

⁷R. Jakubiak, V. P. Tondiglia, L. V. Natarajan, R. L. Sutherland, P. Lloyd, T. J. Bunning, and R. Vaia, *Adv. Mater. (Weinheim, Ger.)* **17**, 2807 (2005).

⁸D. Luo, X. W. Sun, H. T. Dai, Y. J. Liu, H. Z. Yang, and W. Ji, *Appl. Phys. Lett.* **95**, 151115 (2009).

⁹D. Luo, X. W. Sun, H. T. Dai, H. V. Demir, H. Z. Yang, and W. Ji, *J. Appl. Phys.* **108**, 013106 (2010).

¹⁰K. Sakoda, *Opt. Express* **4**, 167 (1999).

¹¹D. E. Lucchetta, L. Criante, O. Francescangeli, and F. Simoni, *Appl. Phys. Lett.* **84**, 837 (2004).

¹²D. E. Lucchetta, L. Criante, O. Francescangeli, and F. Simoni, *Mol. Cryst. Liq. Cryst.* **441**, 97 (2005).

¹³V. K. S. Hsiao, C. Lu, G. S. He, M. Pan, A. N. Cartwright, P. N. Prasad, R. Jakubiak, R. A. Vaia, and T. J. Bunning, *Opt. Express* **13**, 3787 (2005).

¹⁴R. L. Sutherland, L. V. Natarajan, V. P. Tondiglia, and T. J. Bunning, *Chem. Mater.* **5**, 1533 (1993).

¹⁵M. B. Christensen, A. Kristensen, S. Xiao, and N. A. Mortensen, *Appl. Phys. Lett.* **93**, 231101 (2008).

¹⁶M. Notomi, *Phys. Rev. B* **62**, 10696 (2000).